J Mater Sci (2007) 42:1285–1292
DOI 10.1007/s10853-006-1396-6

Composite formation of Thiol-capped Au nanoparticles and mesoporous silica prepared by a sol-gel method

Y. Tai · M. Watanabe · J. Murakami ·
K. Tajiri

Received: 21 May 2004 / Accepted: 13 January 2006 / Published online: 24 January 2007

Abstract We have previously reported the fabrication of a nanocomposite from dodecanethiol-capped Au nanoparticles (average diameter 2.6 nm) and a silica aerogel. It was found that the Au particles were efficiently adsorbed on a silica wet-gel in organic solvents. In this paper, surface analysis of the silica surface and evaluation of adsorption rates for various solvents, performed to elucidate the nature of the interaction between the capped nanoparticles and the silica gel, are described. These observations indicate that dipole-induced dipole interaction between OH groups on the silica surface and metal cores of the nanoparticles is probably important for the adsorption. It was demonstrated that, by changing the solvent polarity, spatial distribution of the nanoparticles inside the gel can be controlled.

Introduction

Chemical and physical properties of small metal particles have been the subject of intensive research because of their scientific and technological importance. It is now well recognized that the properties greatly differ depending on the particle size. For example, chemical reactivity of some metals is enhanced when they take a form of fine particles. Even gold, the least reactive metal, can catalyze chemical reactions when the diameter is less than ≈10 nm [1]. When the sizes of metal particles become even smaller down to sub-nano scales, their chemical reactivities differ by orders of magnitude depending on the number of constituent atoms of the particles as proved from gas-phase studies [2–4].

The above examples suggest that, for fabricating a material with characteristic properties of metal nanoparticles, it is important to assemble nanoparticles in such a way that they preserve their original sizes. For this, it is needed to keep the particles isolated from each other and fix them on surfaces or in inner space of a support. For maximizing the number density of the particles, support materials with large surface area are desired. From this point of view, aerogel is a material with unique potential advantages. Aerogel is a very porous material with a large surface area, which is prepared by polymerization of monomer or oligomer metal alkoxides followed by drying under supercritical conditions [5]. The pore size (1~100 nm) and the porosity of the gels can be controlled by preparation conditions such as the concentration of starting materials and the pH of a reaction system [5].

In our previous letter, we reported that thiol-capped Au nanoparticles are efficiently adsorbed on a silica wet-gel in organic solvents like toluene [6]. The Au particles were immobilized on the silica structure to such an extent that they are not flushed out upon supercritical CO_2 (sc-CO_2: critical points, $T_c = 304.2$ K, $P_c = 7.38$ MPa) drying. Furthermore, since the sc-CO_2 drying

---

Y. Tai (✉) · M. Watanabe · J. Murakami ·
K. Tajiri
Chubu Research Base, National Institute of Advanced Industrial Science and Technology (AIST), Nagoya 463-8560, Japan
e-mail: tai.y@aist.go.jp

Present Address:
M. Watanabe
Toyota Motor Corporation, Toyota City, Japan

is carried out at temperatures only slightly higher than room temperature, diffusion and aggregation of the metal cores could be avoided. By recent progresses in the surfactant-passivation methods, isolated nanoparticles of various elements like noble metals [7, 8], transition metals [9, 10], and metal oxides [11, 12] etc. with a minimum core size as small as 1 nm have been synthesized [13, 14]. Silica aerogel may also be a good support for these nanoparticles.

In this report, we will present full results on the study of the adsorption of dodecanethiol-capped Au nanoparticles ($Au_x(DDT)_y$) on the mesoporous silica surface, and discuss the adsorption mechanism. From qualitative evaluation of adsorption rates in various solvents and surface analyses, it is suggested that dipolar interaction between the surface OH groups and metal cores of the nanoparticles are possibly important. A simple method for controlling the spatial distribution of the Au nanoparticles in a bulk gel will also be described.

Experimental

$Au_x(DDT)_y$ was prepared according to the method of Brust et al. [7]. Briefly, $AuCl_4^-$ ion was extracted from a water to a toluene phase by excess tetraoctylammonium bromide and reduced with sodium borohydride in the presence of dodecanethiol. The molar ratio of Au and dodecanethiol was 1:1~1:3. The product was washed with ethanol and purified two times by recrystallization from toluene/ethanol mixed solvent (1:40 in volume) at 255 K [7].

Silica wet-gel was synthesized by hydrolysis and subsequent condensation of tetramethoxysilane (TMOS) in methanol by using ammonia catalyst: one mole of TMOS was dissolved in 10 moles of methanol, and a 0.1 N NH_4OH solution containing 6 moles of water was added to the solution [5]. A jelly-like bulk solid was formed in a tubular mold (inner diameter: 30 mm, height: 10 mm) by gelation within a few hours. The product was kept in the mold typically for one day at room temperature and then took out from the mold and washed with ethanol.

Adsorption of the nanoparticles on the gel was performed by immersing it in the nanoparticle solutions. Before the immersion, the pore-filling solvent of the gel, ethanol originally, was exchanged to a solvent of the nanoparticle solution: the gel was first soaked in the 1:1 mixture of ethanol and the solvent and then soaked in the solvent for two times. Each step was performed with intervals more than a day.

Drying of the wet-gel by sc-CO_2 was performed as follows. The wet-gel was placed in an autoclave with pore-filling toluene solvent, and CO_2 was fed into the autoclave. To substitute the solvent for liquid CO_2, the pressure of CO_2 was then raised to above 7 MPa by using a high pressure pump and kept for 2 h, allowing a small amount of CO_2 to flow out of the autoclave with toluene. This operation was done for three times to complete the substitution. The ambient temperature was kept below 297 K during the procedure. CO_2 was then removed under supercritical conditions: the vessel temperature and pressure were above 313 K and 8 MPa, respectively.

Transmission electron microscopy (TEM) images of the nanoparticles were taken by the JOEL 2010 microscope with a LaB_6 filament operated at 200 kV. For the TEM observations, $Au_x(DDT)_y$-toluene solution or ethanol dispersion of a ground nanocomposite gel was dried on a carbon film.

UV–vis. spectra of the nanoparticle solutions were recorded using the JASCO V-570 or the Perkin-Elmer Lambda-18 spectrometer with the transmission mode. IR spectra were obtained by the JASCO FT/IR-620 spectrometer for powdered silica sandwiched between KBr plates.

Elemental analyses of the nanoparticles were performed using the Shimadzu lab center XRF-1700 X-ray fluorescence spectrometer.

Results and discussion

Adsorption of Au nanoparticles on mesoporous silica

Figure 1a–c show photographs of a wet-gel immersed in $Au_x(DDT)_y$ (average diameter 2.6 nm)–toluene solution [6]. 3.0 mg of $Au_x(DDT)_y$ was dissolved in 50 ml of toluene ($\approx 5 \times 10^{-4}$ mmol). The diameter and the thickness of the gel were 40 and 10 mm, respectively. Initially, the gel was transparent (Fig. 1a), and gradually became as colored as the solution (Fig. 1b). The gel finally became dark colored and the solution in turn transparent, indicating all the Au particles were incorporated in the gel (Fig. 1c).

In Fig. 2 we show a TEM image (a) and the corresponding core size distribution (b) of the as-prepared Au nanoparticles. The average core diameter was 2.6 nm, and thus, the total particle size is ≈5.2 nm if the thiol chains take the all-trans conformation. On the other hand, the size of the mesopores of the aerogel measured by the N_2 adsorption method gave a maximum around 15 nm. In the wet-gel, pores

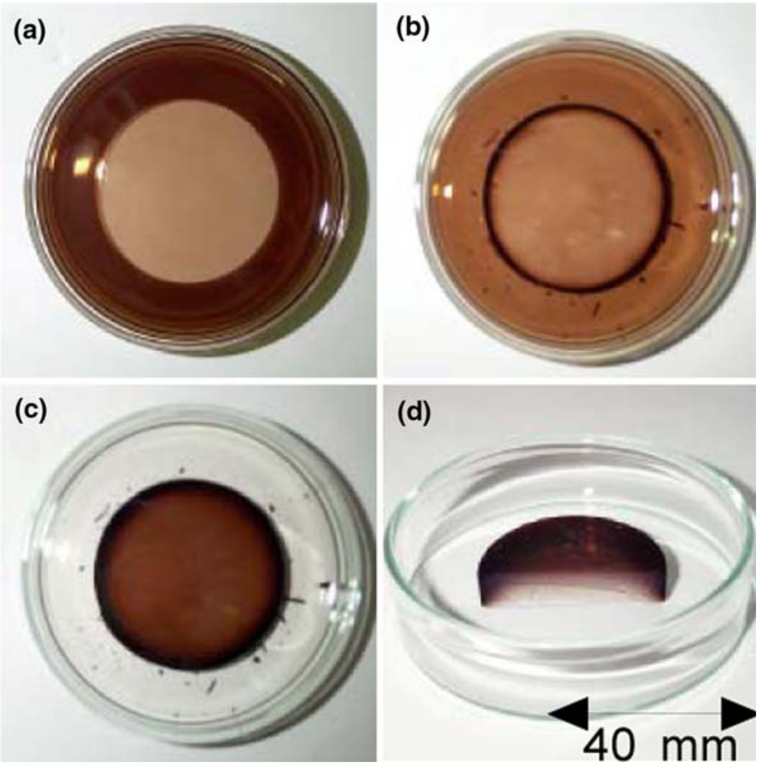

Fig. 1 Photographic images of silica wet-gel in the $Au_x(DDT)_y$–toluene solution at (**a**) 0, (**b**) 5, and (**c**) 57 h after immersion. (**d**) A photographic image of the $Au_x(DDT)_y$/silica composite aerogel. The product aerogel was cut into two to show the spatial distribution of the nanoparticles

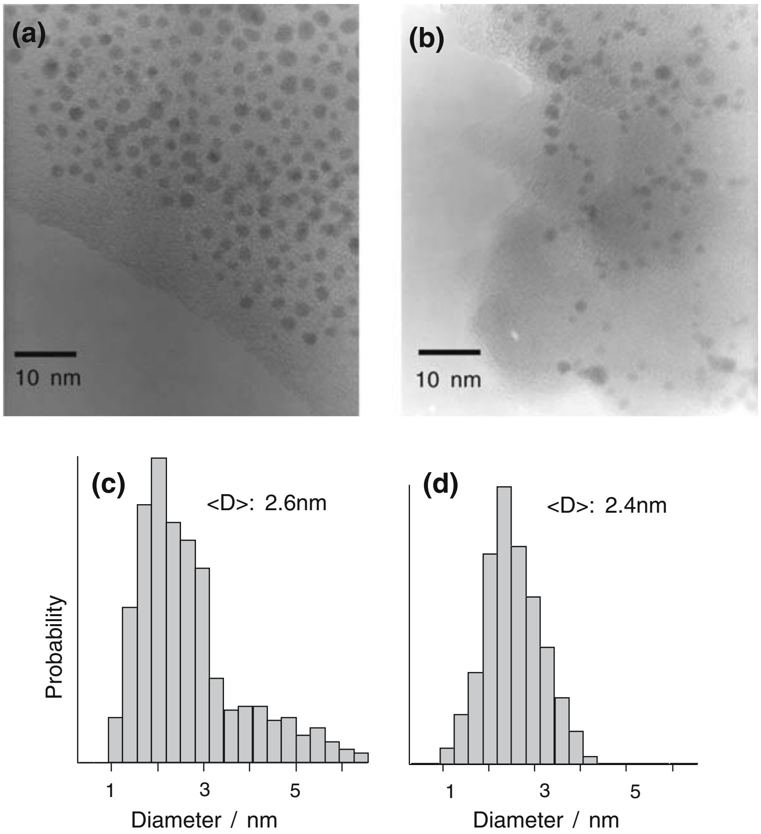

Fig. 2 TEM image and the corresponding core size distribution of the as-prepared $Au_x(DDT)_y$ nanoparticles (**a, c**) and of the $Au_x(DDT)_y$ particles in the composite aerogel (**b, d**). The core size distributions were obtained by measuring the diameters of 200~300 particles in the TEM images

are expected to have a similar size distribution to that in the aerogel. Considering that thiol chains are flexible to some extent, it is expected that the Au nanoparticles easily diffuse into the mesopores.

The wet-gel composite, incorporating the Au particles, was dried in air and in sc-CO_2. Drying in air gave rise to considerable shrinkage of the gel, yielding a composite xerogel: the volume reduced to ≈1/4 of the original one. The UV–vis. spectra of the composites obtained by drying in air and in sc-CO_2 were both similar to that of the $Au_x(DDT)_y$ solution [6]. This implies that fusion or fragmentation of the particles during the composite formation and the drying processes do not occur.

Figure 1d shows a photograph of a composite aerogel. The density of the composite was ≈0.2 g/cm^3. The particle size distribution in the composite shown in Fig. 2d was almost identical to that of the original $Au_x(DDT)_y$ (Fig. 2c). From elemental analysis, it was found that the molar ratio of Au to S for $Au_x(DDT)_y$ solid, xero- and aerogel composites were the same within errors. These observations further support that the structure and the composition of the Au nanoparticles were not affected by the adsorption and the drying processes. Drying by sc-CO_2 can be performed at temperatures slightly above room temperature: in the present case, the temperature in the autoclave were kept lower than 343 K. This temperature is well below the temperature at which the thiol molecules desorb from the metallic core [15]. Moreover, it is expected that the adsorbed $Au_x(DDT)_y$ particles are not very mobile in the silica gel at such a temperature, as evidenced by visual inspection. It indicated that the spatial distributions of the nanoparticles in the wet-gel and the aerogel are similar.

The Au content in the composite aerogel in the Fig. 1d is 0.18 wt%. We used a dilute solution for the visual inspection of the gels and the solution in Fig. 1. Our investigation on the amount of Au supported in the gel using more concentrated solutions showed that the Au content up to ≈25 wt% can be achieved.

Evaluation of adsorption rates in various conditions

To clarify the nature of the adsorption mechanism of the Au nanoparticles on the silica surface, the adsorption rate was assessed for various solvents. Figure 3 shows the changes in the optical absorbance of a nanoparticle-containing solution after the wet-gel was immersed in it. The inset in Fig. 3a shows a sketch of the UV–vis. absorbance measurement. A cylindrical gel (φ7.8 mm × length 8.0 mm) with pores filled with neat toluene was put in the toluene solution of $Au_x(DDT)_y$ in a quartz cell with a screw cap. Particle concentration in the solution was 0.083 g/L. At this concentration, the number of the adsorption sites in the gel is far beyond the number of particles in the solution [16]. The optical absorption spectrum of the solution was measured using a light beam from a halogen lamp passing more than 1 mm above the gel. The UV–vis. spectrum showed a broad absorption band (plasmon band) around 515 nm superimposed on absorption bands due to inter and intra band transitions [8]. Figure 3a shows a series of absorption spectra, showing the absorbance of the solution decreases with time. Figure 3b shows the change in the absorbance at 300, 500, and 600 nm with time. Due to the adsorption of the nanoparticles, the absorbances decreased with time after the immersion. Changes in

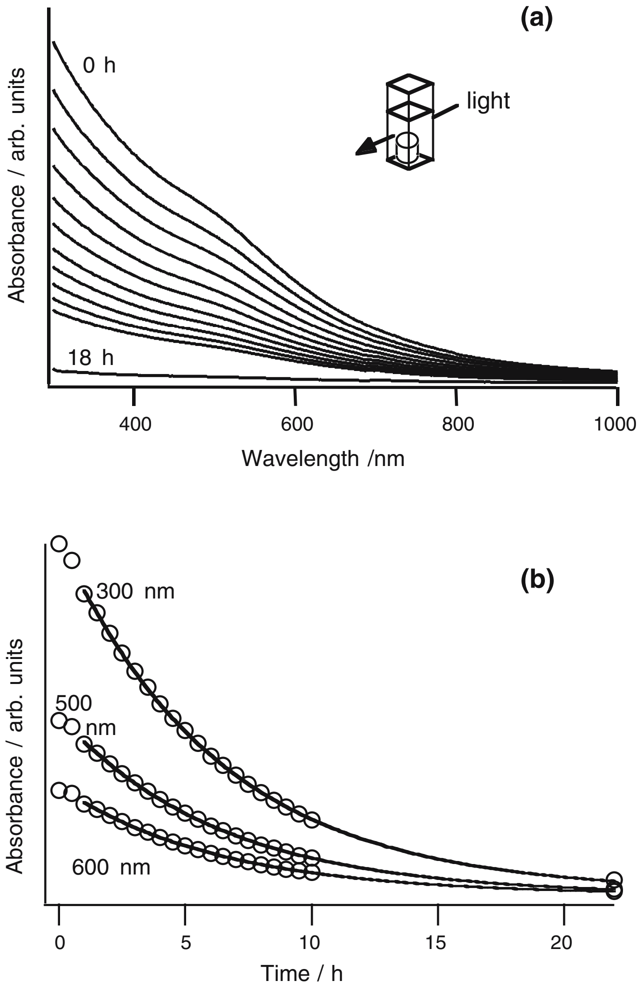

Fig. 3 Changes of UV–vis. absorption spectra (**a**) and in absorbance at three different wavelengths with time (**b**) of the $Au_x(DDT)_y$–toluene solution in the presence of silica wet-gel. The inset in (**a**) shows a sketch of the absorbance measurement

absorbance with time were dependent on various conditions such as solvent polarity, surface hydrophobicity, and nanoparticle size, and thus, were used for qualitative understanding of the nanoparticle—surface interactions.

Figure 4a shows changes in optical absorbance at 500 nm with time in toluene, Tetrahydrofuran (THF) and mixed solvents of THF or ethanol and toluene. The average diameter of Au core of the nanoparticles is 2.6 nm.

Apart from the data for the pure toluene solvent, the decrease in the absorbance showed a general trend that the absorbance rapidly decreased from 0.7 to ≈0.6 in about 10 h and then decreased gradually. The decrease in the first 10 h coincides with the increase of the solvents due to the addition of the wet-gels containing neat solvents if we assume that the nanoparticles are homogeneously distributed in the cell. Thus, the decrease of the absorbance in the first 10 h are considered not to be due to the adsorption of the nanoparticles on silica but to the diffusion of the particles to homogenize the particle concentration in the cell. The adsorption or trapping of the nanoparticles on the silica surface is probably the rate-determining process for the decrease of the absorbances after 10 h. This is consistent with the spatial distribution of the adsorbed particles in the gel, which will be shown in Fig. 7. The adsorbed particles were almost homogeneously distributed in the gel in THF and the 1:1 mixed solvents, while in the neat toluene, the particles were adsorbed only on the peripheral parts on the gel. In toluene, diffusion of the nanoparticles may be the rate-determining process. Further information on the diffusion of the nanoparticles would be acquired from the dynamic light scattering (DLS) measurement.

As can be seen in Fig. 4a, mixing THF with toluene led to decrease in the adsorption rate. By mixing only 10 vol.% of THF with toluene, breaching time, the time at which the original absorbance decreases to the half, was elongated by ≈10 times. Moreover, for the THF solvent, the optical absorbance was equilibrated around 0.4. This value corresponds to the amount of supported Au nanoparticles is ≈0.09 mg. In the toluene solvent, it was deduced from a rough evaluation of the adsorption isotherm that ≈24 mg of Au nanoparticles can be adsorbed on silica at the same equilibrated concentration. It is, therefore, considered that the interaction between the nanoparticles and the silica surface is much weakened in THF. These data seem to suggest that electric interactions at the interface of the nanoparticles and silica are important for the nanoparticle adsorption, taking the dielectric constants of the solvents (toluene: 2.36, THF: 7.8 at 298 K) into account. However, in liquid-phase, solubility of an adsorbate is known to affect the adsorbate–surface interactions [17]: if solubility is high, adsorbates tend to stay in liquid phase. The solubilities of the present Au$_x$(DDT)$_y$ particles in toluene and THF are not known. Thus, the reduction of the adsorption rate by mixing THF in toluene may be due to enhanced solubility of the Au$_x$(DDT)$_y$ particles in the mixed solvents. To clarify whether this effect is important, toluene was mixed with ethanol in which the Au$_x$(DDT)$_y$ particles are not soluble. Solid circles in Fig. 4a show the change in absorbance of 1:1 mixed solution of toluene and ethanol (ε(298 K) = 24.3),

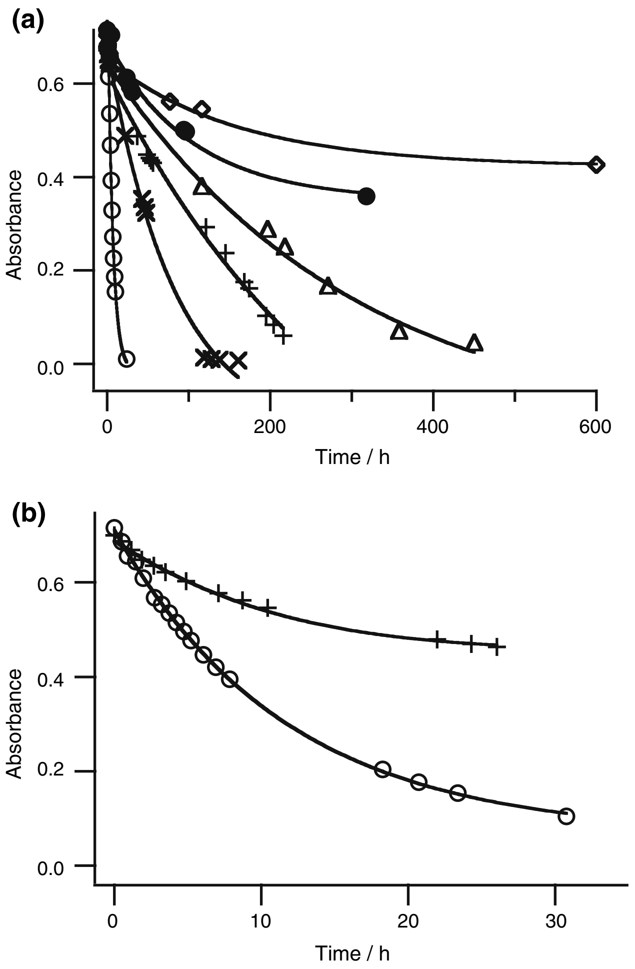

Fig. 4 (**a**) Changes in absorbance at 500 nm with time for the Au$_x$(DDT)$_y$ solutions with various solvents: (○) toluene, (×) toluene: THF = 9:1, (+) toluene: THF = 7:3, (△) toluene: THF = 5:5, (•) toluene:ethanol = 5:5, (◇) THF. (**b**) Time dependence of UV–vis. absorbance in toluene for Au$_x$(DDT)$_y$ with two different size: (○) 3 nm, (+) 1.5 nm. Note the adsorption rates cannot be compared between different figures since the pore sizes of the gels used for experiments for Figs. 3, 4a, b are probably not the same from one another because of different aging times

which clearly indicates that the adsorption rate is similarly reduced. Hence, we consider that the reduction of the adsorption rate is mainly caused by the mixed molecules weakening the interaction between the nanoparticles and the surface. It is probable that polar molecules gather around OH groups on a silica surface and block adsorption sites [18].

It is considered that there are two possible mechanisms that electric interactions at the interface play a role for the adsorption of the nanoparticles onto the silica surface. One is the dipole–dipole interaction between the OH groups of silica and thiol layers of the nanoparticles. In the Au nanoparticles, surrounding thiol molecules probably form a dipole-layer ($R^+–S^-$) which is analogous to that in self-assembled thiol monolayers on a Au surface [19]. Thus, the dipole–dipole interaction between the OH groups and the thiol layer may anchor the particles on the surface. The other is the dipole-induced dipole interaction between the OH groups and the nanoparticles. The nanoparticles contain highly polarizable Au cores; thus, their interactions may dominate.

To clarify which interaction is responsible for the nanoparticle adsorption, adsorption of nanoparticles with two different sizes was investigated. Figure 4b compares the adsorption rates of nanoparticles with average core size of 3 and 1.5 nm. The core size was controlled by changing temperature for the particle preparations. As can be seen, the larger particles are more rapidly adsorbed on the silica surface; the adsorption rate was about 2~4 times larger for the larger particles.

It is reported that a dodecanethiol molecule occupy almost the same surface area on a nanoparticle to that on an Au(111) surface (≈22 Å^2) [20]. Since the value is dependent on the property of the gold surface and the thiol molecules, it is expected that the density of thiols on the nanoparticle surfaces is not very different for the particles with core diameters of 1.5 and 3 nm. Thus, polarization of the metal cores, dependent on the volume, is considered to be important for the nanoparticle adsorption.

Surface analysis of the silica gel

In general, on silica surfaces, uncondensed hydroxyl groups remain and give them polar properties [21]. In the present study, however, these hydroxyl groups can be substituted by ethoxy groups by an esterification reaction since we used ethanol as an original pore filling solvent after the silica gels were prepared. Moreover, there is a possibility that unreacted methoxy groups of TMOS, the starting reagent, remain on the surface. Thus, to clarify which surface species is dominant and responsible for the adsorption of the Au nanoparticles, IR spectroscopy was performed for the gel dried in air (spectrum (a) in Fig. 5). At ≈1,090 and ≈1,210 cm^{-1}, the Si–O–Si stretching vibrations are seen [5]. The broad absorption band around 3,400 cm^{-1} is due to the OH stretching vibrations of surface OH groups and adsorbed water molecules. The CH stretching vibration due to ethoxy or methoxy groups, expected at ≈2,900 cm^{-1} [5], is not obvious in the spectrum (a). Spectrum (b) in Fig. 5 is for a surface modified silica gel prepared by means of a coupling reaction of the OH groups and hexamethyldisilazane (HMDS): a wet-gel was soaked for 2 h in neat HMDS [22] and then washed with ethanol for several times.

$$\begin{aligned} &\equiv \mathrm{Si{-}{-}OH} + 1/2((\mathrm{CH_3})_3\mathrm{Si})_2\mathrm{NH} \rightarrow \\ &\equiv \mathrm{Si{-}{-}O{-}{-}Si(CH_3)_3} + 1/2\mathrm{NH_3} \end{aligned} \tag{1}$$

The intensity of the OH stretching mode (3,400 cm^{-1}) was reduced and the CH stretching mode (2,900 cm^{-1}) became apparent. These results suggest, though qualitatively, OH groups are dominant on the silica surface.

Effect of hydrophobization of the silica surface on adsorption

To confirm the importance of the surface OH groups on the adsorption, we have tested the adsorption of the $Au_x(DDT)_y$ particles on the silica modified by HMDS. Figure 6 compares the adsorption of the particles on modified and unmodified silica (5 g of

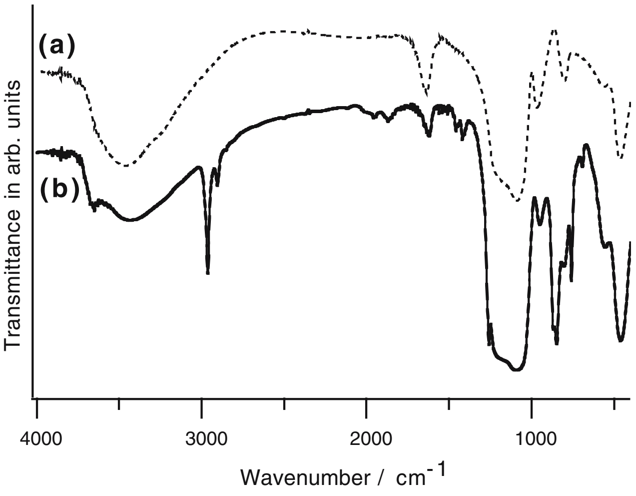

Fig. 5 IR spectra for (**a**) silica xerogel and (**b**) xerogel modified with HMDS

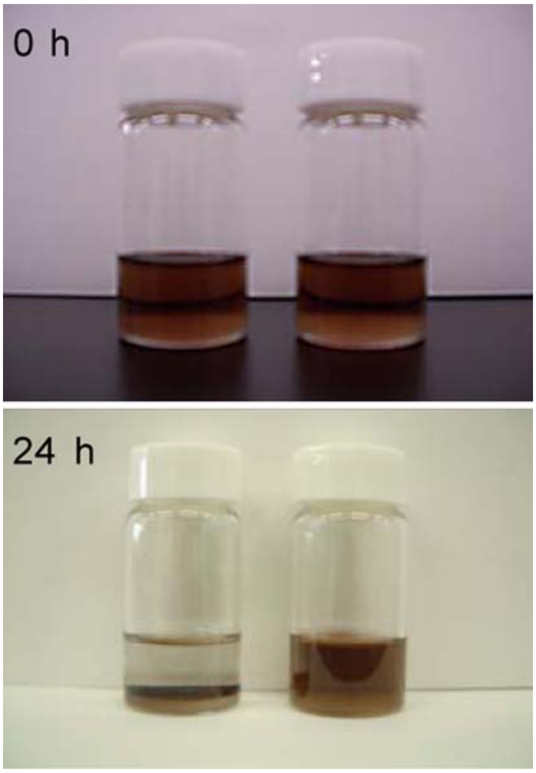

Fig. 6 Effect of surface modification by HDMS on adsorption of the $Au_x(DDT)_y$ particles. Modified (right) and unmodified (left) silica powders are immersed in toluene solution of the $Au_x(DDT)_y$ particles

silica gel powder of 60~80 mesh, Kanto Chemical inc.) immersed in the toluene solution of $Au_x(DDT)_y$ with a concentration of 0.06 g/L. In 24 h of the immersion, the solution loaded with the unmodified silica gel powder became almost transparent while the color of the solution with the modified silica powder was as dark as the starting solution. From this result, we conclude that the surface OH groups form adsorption sites for the particles.

Spatial distribution of the $Au_x(DDT)_y$ particles inside the bulk silica gel

Spatial distribution of the $Au_x(DDT)_y$ particles inside the bulk silica gel was investigated for the composite wet-gels formed in various solutions. Figure 7 compares sectional views of the composites formed in THF, toluene, and THF/toluene (1:1) mixed solution. Each composite wet-gel disk (φ30 mm × thickness 10 mm) was sliced along a bisector of the base of the disk. As seen in the figure, spatial distributions of the particles are very different among one another: the distribution in the gel formed in THF is almost homogeneous, whereas in the composite gel formed in toluene the particles exist only in the peripheral part of it. In the gel formed in the THF/toluene (1:1) mixed solution, The distribution is almost homogeneous, while there exists a weak gradient in the spatial distributions of the particles: the particle density is higher in the peripheral part. In toluene, the electrostatic interactions between the thiol chains and the surface OH groups are large and thus the nanoparticles approaching to the periphery of the bulk gel would be immediately trapped on the adsorption sites. In contrast, in polar solvents like THF, the interaction is greatly depressed. As a result, the particles distribute homogeneously in the gel before they are adsorbed on the gel surface. These results indicate that the spatial distribution of the particles inside the gels can be controlled by only changing the polarity of the solvents.

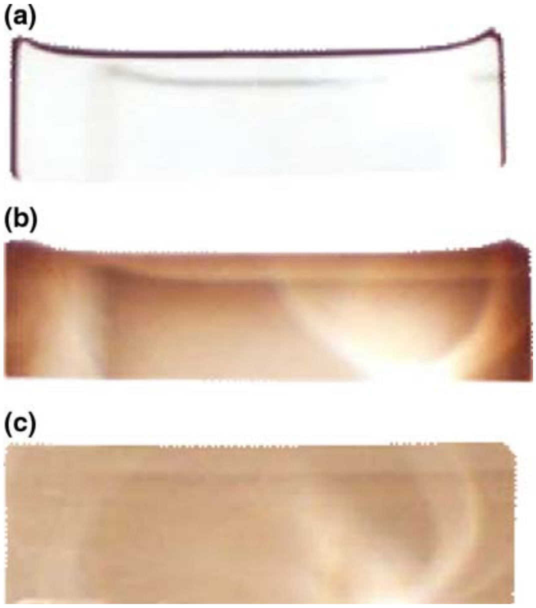

Fig. 7 Sectional view of the composite wet-gels formed in (**a**) toluene, and (**b**) THF/toluene (1:1) and (**c**) THF

Conclusion

We have found that $Au_x(DDT)_y$ particles were efficiently adsorbed on a silica wet-gel in nonpolar organic solvents and the particles were not flushed out during supercritical CO_2 drying. From the evaluation of adsorption rates in various conditions and surface analysis, it is suggested that the dipole-induced dipole interaction between OH groups on the silica surface and the nanoparticles are probably important for the adsorption. It was also shown that by changing the polarity of the solvents, spatial distribution of the particles inside the gels can be controlled.

Acknowledgements The authors are grateful to Prof. T. Tanji of Nagoya University and Prof. K. Kaneko of Kyushu University for TEM observations, to Dr. M. Tazawa for his help in measuring IR spectra, and to Dr. F. Ohashi for elemental analyses. Dr. T. Miki is acknowledged for his help and advice in preparing $Au_x(DDT)_y$ particles. This work was partly supported by the core research for evolutional science and technology (CREST) conducted by Japan Science and Technology Corporation (JST). The authors are also grateful to Nippon Sheet Glass Foundation for Materials Science and Engineering for financial support.

References

1. Haruta M (1997) Catal Today 36:153
2. Richtsmeier SC, Parks EK, Liu K, Pobo LG, Reily SJ (1985) J Chem Phys 82:3659
3. Alford JM, Laaksonen RT, Smalley RE (1991) J Chem Phys 94:2618
4. Holmgren L, Andersson M, Rosen A (1998) J Chem Phys 109:3232
5. Brinker CJ, Scherer GW (1990) Sol-gel science Ch. 3 and 9. Academic press, San Diego
6. Tai Y, Watanabe M, Kaneko K, Tanemura S, Miki T, Murakami J, Tajiri K (2001) Adv Mater 13:1611
7. Brust M, Walker M, Bethell D, Schiffrin DJ, Whyman R (1994) J Chem Soc Chem Commun 801
8. Sarathy KV, Raina G, Yadev RT, Kulkarni GU, Rao CNR (1997) J Phys Chem B101:9876
9. Wagener M, Guenther B, Blums E (1999) J Magn Magn Mater 201:18
10. Sun S, Murray CB (1999) J Appl Phys 85:4325
11. Connor CJO, Seip CT, Carpenter EE, Li S, John VT (1999) Nanostruct Mater 12:65
12. Li M, Schnablegger H, Mann S (1999) Nature 402:393
13. Schaaff TG, Shafigullin MN, Khoury JT, Vezmar I, Whetten RL, Cullen WG, First PN, Gutierrez-Wing C, Ascensio J, Jose-Yacaman MJ (1997) J Phys Chem B101:7885
14. Yonezawa T, Yasui K, Kimizuka N (2001) Langmuir 17:271
15. Hostetler MJ, Wingate JE, Zhong CJ, Harris JE, Vachet RW, Clark MR, Londono JD, Green SJ, Stokes JJ, Wignall GD, Glish GL, Porter MD, Evans ND, Murray RW (1998) Langmuir 14:17
16. The amount of the adsorbed particles under the complete coverage conditions was evaluated as ≈24 mg (W_{max}) for the gel of the present size. The volume of the qualtz cell is ≈3 ml; thus, the amount of the particles in the cell is at most 0.25 mg. This value is much smaller than W_{max}
17. Adamson AW (1960) Physical chemistry of surfaces ch. 8. Interscience Publishers, a division of John Wiley and Sons New York
18. Iler RK (1979) The chemistry of silica ch. 6. Wiley Interscience Publication, John Wiley and Sons, New York
19. Lue J, Delamarche E, Eng L, Bennewitz R, Meyer E, Guentherodt H-J (1999) Langmuir 15:8184
20. Yonezawa T, Onoue S, Kunitake T (1999) Polym Prepr Jpn 48:3547
21. Scott RPW (1993) Silica gel and bonded phases – their production, properties and use in LC – Ch. 4 and 6. John Wiley and Sons, Chichester
22. Belyakova LA, Varvarin AM (1999) Colloids Surf A Physicochem Eng Asp 154:285